Dynamics of energy transfer and frequency upconversion in Tm 3 + doped fluoroindate glass

Vladimir A. Jerez, Cid B. de Araújo, and Y. Messaddeq

Citation: Journal of Applied Physics **96**, 2530 (2004); doi: 10.1063/1.1769596
View online: http://dx.doi.org/10.1063/1.1769596
View Table of Contents: http://scitation.aip.org/content/aip/journal/jap/96/5?ver=pdfcov
Published by the AIP Publishing

Dynamics of energy transfer and frequency upconversion in Tm^{3+} doped fluoroindate glass

Vladimir A. Jerez and Cid B. de Araújo[a)]
Departamento de Fisica Universidade Federal de Pernambuco 50670-901 Recife, PE, Brazil

Y. Messaddeq
Instituto de Química Universidade do Estado de São Paulo 14800-900 Araraquara, SP, Brazil

(Received 29 September 2003; accepted 19 May 2004)

Blue and ultraviolet upconversion (UC) emissions at 455 and 363 nm were observed from Tm^{3+} doped fluoroindate glasses pumped at 650 nm. The time behavior of the UC signals was studied for different Tm^{3+} concentrations. The measurements revealed the origin of the UC process as well as allowed to quantify the interaction between Tm^{3+} ions. The results indicate that a two-step one-photon absorption process is responsible for the UC emissions, and dipole-dipole interaction provides the main contribution for energy transfer (ET) among active ions. The critical distance between Tm^{3+} ions at which the ET rate is equal to the decay rate of noninteracting Tm^{3+} ions was determined. © *2004 American Institute of Physics*. [DOI: 10.1063/1.1769596]

I. INTRODUCTION

The optical properties of rare earth (RE) doped solids have been extensively investigated.[1,2] However, the search for new materials with improved functionality is still an active area. In particular, the investigation of optimized glasses for efficient lasing and frequency upconversion (UC) processes requires more effort due to their potential applications.[1,2]

Amongst the enormous variety of existing glasses, fluoride systems are attractive materials for photonics because large amount of RE ions can be introduced in the matrix and they can be used to fabricate special optical fibers and fiber lasers. Moreover, due to cut-off phonons of low energy, the nonradiative relaxation rate of RE excited states in fluoride glasses is small and thus the luminescence efficiency is larger than in other systems. Indeed, it well characterizes the good performance of fluoride glasses in color displays and lasers.

Recently, a class of fluoride systems—fluoroindate glasses (FIG)—has gained attention because a number of improvements in their characteristics were developed.[3] Nowadays, FIG samples can be prepared with good optical quality, large stability against atmospheric moisture, and low optical attenuation from 0.25 μm to 8 μm. Optical properties were studied in a large number of RE-doped FIG samples[3–16] and the results demonstrate the large potential of this material to be used in upconverters, optical amplifiers, lasers, and sensors.

In this article we report on the spectroscopic properties of Tm^{3+}-doped FIG by single wavelength pumping in the red region. The Judd-Ofelt (J-O) theory[17,18] was used to obtain the quantum efficiency of the $4f$-$4f$ transitions and other spectroscopic parameters. The dynamics of the fluorescence was investigated and energy transfer (ET) processes among Tm^{3+} ions were studied. UC from red to blue and ultraviolet was studied and the mechanism which originated the upconverted emissions was elucidated.

UC in Tm^{3+} doped fluoroindate glasses has been previously studied using continuous wave (CW) lasers for excitation.[12] The present report provides different information because different glass compositions were used and because the excitation source is a pulsed laser that allows a better characterization of the dynamics of the UC process.

II. EXPERIMENT

The samples used have the following composition in mol %: $(39-x)InF_3$-$20ZnF_2$-$20SrF_2$-$16BaF_2$-$2GdF_3$-$2NaF$-$1GaF_3$-$xTmF_3$, where $x=1.0$, 2.0, and 3.0. The glass synthesis was implemented using standard proanalysis oxides and fluorides as starting materials following the procedure given in Refs. 3–8. Samples with dimensions $0.2\times1.0\times1.0$ cm^3 were used.

The absorption spectra of the samples were measured

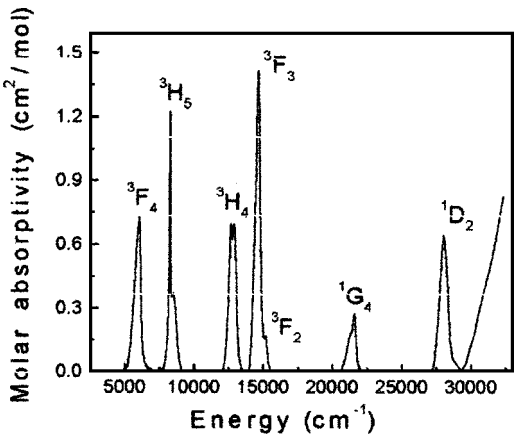

FIG. 1. Absorption spectrum of fluoroindate glass with 1.0 mol % of Tm^{3+} ions.

a)Author to whom correspondence should be addressed; electronic mail: cid@df.ufpe.br

TABLE I. Experimental f_{exp} and theoretical f_{theo} oscillator strengths for transitions originated from the ground multiplet ($^3H_6$).

Excited multiplet	Energy (cm^{-1})	f_{exp} ($\times 10^{-6}$)	f_{theo} ($\times 10^{-6}$)
$^3F_4$	5920	1.79	1.85
$^3H_5$	8320	1.43	1.29
$^3H_4$	12 771	1.92	1.94
$^3F_{3,2}$	14620	2.95	2.98
$^1G_4$	21 445	0.70	0.56
$^1D_2$	28 011	1.91	1.90

using a double-beam spectrophotometer that operates from 400 cm^{-1} (2.5 μm) to 30 000 cm^{-1} (0.33 μm).

The Nd:YAG (YAG—yttrium aluminum garnet) pumped dye laser used for the fluorescence experiments operates at 5 Hz with ≈10 ns pulses, peak power of ≈20 kW, linewidth of ≈0.5 cm^{-1}, and could be tuned over the 620–690 nm range. The linearly polarized dye laser beam was focused into the sample with a 3 cm focal length lens and the fluorescence was collected along a direction perpendicular to the incident beam direction by a 5 cm focal length lens. The signal was processed using a digital oscilloscope connected to a computer.

III. RESULTS AND DISCUSSION

The absorption spectrum of the FIG sample with $x=1.0$ is presented in Fig. 1. The spectra for other samples are similar with no shift in the wavelengths of the absorption peaks. The intensities of the bands vary linearly with the concentration of Tm^{3+}. All transitions are inhomogeneously broadened. Each assignment in Fig. 1 corresponds to the upper level of transitions originating from the Tm^{3+} ground multiplet ($^3H_6$).

TABLE II. Energy gap, radiative transition probabilities $A_{JJ'}$, branching ratios $\beta_{JJ'}$, radiative lifetimes τ_R, and multiphonon relaxation rates W_{MP} of Tm^{3+} ion at room temperature.

Transition	Energy gap (cm^{-1})	A_{JJ} (s^{-1})	$\beta_{JJ'}$	β_{JJ} (exp)	τ_R (μs)	W_{MP} (s^{-1})
$^3F_4 \rightarrow {}^3H_6$	5920	140	1		7117	2.3×10^{-04}
$^3H_5 \rightarrow {}^3F_4$	2400	4	0.025		6170	$3.9\times10^{+04}$
$^3H_6$	8320	157	0.975			5.6×10^{-10}
$^3H_4 \rightarrow {}^3H_5$	4451	16	0.022		1251	6.2×10^{-01}
$^3F_4$	6851	59	0.074			1.5×10^{-06}
$^3H_6$	12 771	722	0.904			2.2×10^{-20}
$^3F_3 \rightarrow {}^3H_4$	2006	2.7	0.002		576	3.2×10^{05}
$^3H_5$	6457	169	0.098			1.2×10^{-05}
$^3F_4$	8857	45	0.026			3.1×10^{-11}
$^3H_6$	14 777	1516	0.874			4.6×10^{-25}
$^3F_2 \rightarrow {}^3F_3$	374	0.0	0.0		1143	$2.1\times10^{+09}$
$^3H_4$	2380	6.2	0.007			$4.3\times10^{+04}$
$^3H_5$	6831	112	0.128			1.7×10^{-06}
$^3F_4$	9231	291	0.333			4.2×10^{-12}
$^3H_6$	15 151	464	0.532			6.1×10^{-26}
$^1G_4 \rightarrow {}^3F_2$	6294	10	0.008		791	3.1×10^{-05}
$^3F_3$	6680	34	0.028			3.8×10^{-06}
$^3H_4$	8674	128.2	0.102			8.4×10^{-11}
$^3H_5$	13 125	435.3	0.345			3.3×10^{-21}
$^3F_4$	15 525	105.3	0.083			8.2×10^{-27}
$^3H_6$	21 445	549.5	0.434			1.2×10^{-40}
$^1D_2 \rightarrow {}^1G_4$	6566	77	0.005		67	7.1×10^{-06}
$^3F_2$	12 860	589	0.044			1.3×10^{-20}
$^3F_3$	13 234	499	0.034			1.8×10^{-21}
$^3H_4$	15 240	674	0.046			3.8×10^{-26}
$^3H_5$	19 691	38	0.003			1.5×10^{-36}
22 09 $^3F_4$	220 91	7031	0.477	0.544		3.7×10^{-42}
$^3H_6$	28 011	5836	0.396	0.350		5.4×10^{-56}

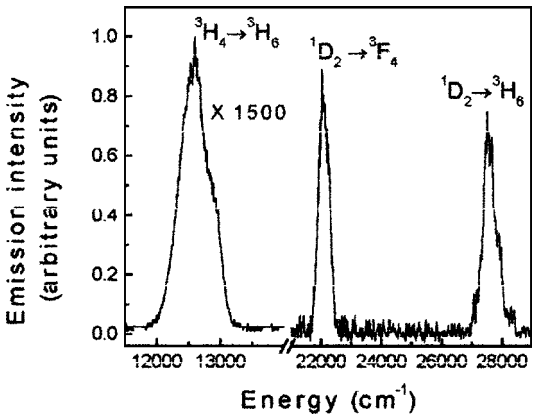

FIG. 2. Emission spectra of Tm^{3+}-doped glass for excitation at 650 nm (sample concentration: $x=1.0$).

The analysis of the absorption spectra was made using the J-O theory.[17,18] From the integrated absorbance spectra three intensity parameters, which are dependent on the ligand field and dominate the transition probabilities in the glass, were determined: $\Omega_2=2.36\times10^{-20}$ cm^2, $\Omega_4=1.59\times10^{-20}$ cm^2, and $\Omega_6=1.21\times10^{-20}$ cm^2. Oscillator strengths for transitions originating from the ground multiplet are given in Table I. Branching ratios, radiative lifetimes, and multiphonon relaxation rates were determined for all Tm^{3+} levels and the results are presented in Table II. The procedure to calculate the quantities given in Table I and Table II is based on Refs. 17 and 18 except for the multiphonon relaxation rates which were calculated using the "energy gap law"[19] considering the energy of the cut-off phonon mode of the FIG matrix (≈500 cm^{-1}).[20]

The fluorescence spectrum with transition $^3H_6 \rightarrow {}^3F_2$ being resonantly excited at 650 nm (15 385cm^{-1}) is shown in Fig. 2. The emitted intensities at ≈22 000 cm^{-1} (≈455 nm) and 27 550 cm^{-1} (≈363 nm) have the same order of magnitude. The intensity at ≈12 500 cm^{-1} (≈800 nm) was attenuated 1500 times to be included in the

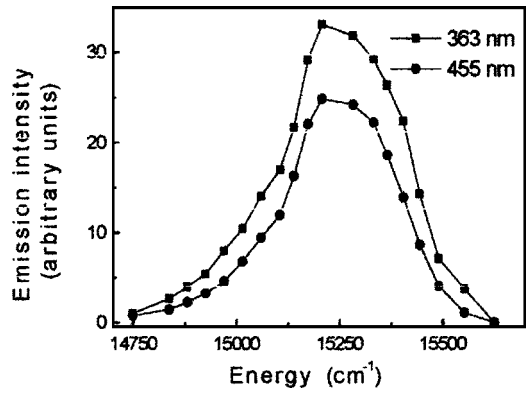

FIG. 3. Excitation spectra of UC emissions. Points represent experimental results. The solid line is a guide to the eyes (sample concentration: $x=1.0$).

TABLE III. Decay times τ_D of the excited multiples $^1D_2$ and $^3H_4$.

x	$\tau_D(\mu s)$
$^1D_2$ multiplet	
1.0	26
2.0	13
3.0	6
$^3H_4$ multiplet	
1.0	560
2.0	139
3.0	44

same figure. The fluorescence intensity at ≈800 nm vary linearly with the laser intensity while the emissions at 455 nm and 363 nm show a quadratic dependence. The intensity of the fluorescence bands vary linearly with the Tm^{3+} concentration. The emission at ≈800 nm is attributed to transition $^3H_4 \rightarrow {}^3H_6$ that occurs after phonon-assisted decay from $^3F_2$ to $^3H_4$. The blue and ultraviolet emissions are attributed to transitions $^1D_2 \rightarrow {}^3F_4$ and $^1D_2 \rightarrow {}^3H_6$, respectively. The calculated branching ratio of the 455 and 363 nm transitions given in Table II are comparable, in agreement with the spectrum of Fig. 2. Blue emission corresponding to $^1G_4 \rightarrow {}^3H_6$ is not observed in this case because the multiphonon relaxation rate from $^1D_2$ to $^1G_4$ is small. Also, because of the laser pulse duration (≈10 ns), excitation from $^3F_4$ to $^1G_4$ is not effective as a CW experiments.[12,21]

Figure 3 shows the excitation spectra of the UC emissions. Note that both intensities are maximized when the dye laser wavelength is in resonance with transition $^3H_6 \rightarrow {}^3F_2$. No UC emission is observed when the laser is tuned to transition $^3H_6 \rightarrow {}^3F_3$.

The fluorescence bands show a nonexponential temporal decay for the three samples. Values of rise time in the range 150–316 ns were measured for transition $^3H_4 \rightarrow {}^3H_6$ with decay time varying from 560 to 44 μs, as presented in Table III. The rise time of the UC transitions follows the laser pulse rise time for all samples while the decay time decreases from 26 to 6 μs as the Tm^{3+} concentration increases.

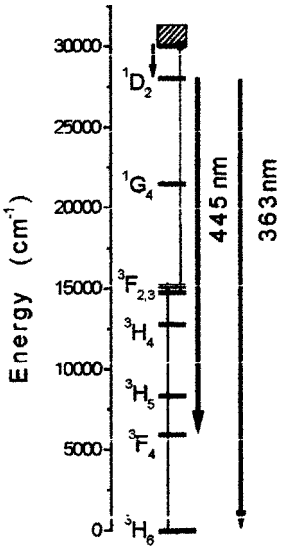

FIG. 4. Excitation routes for UC emissions at 455 and 363 nm.

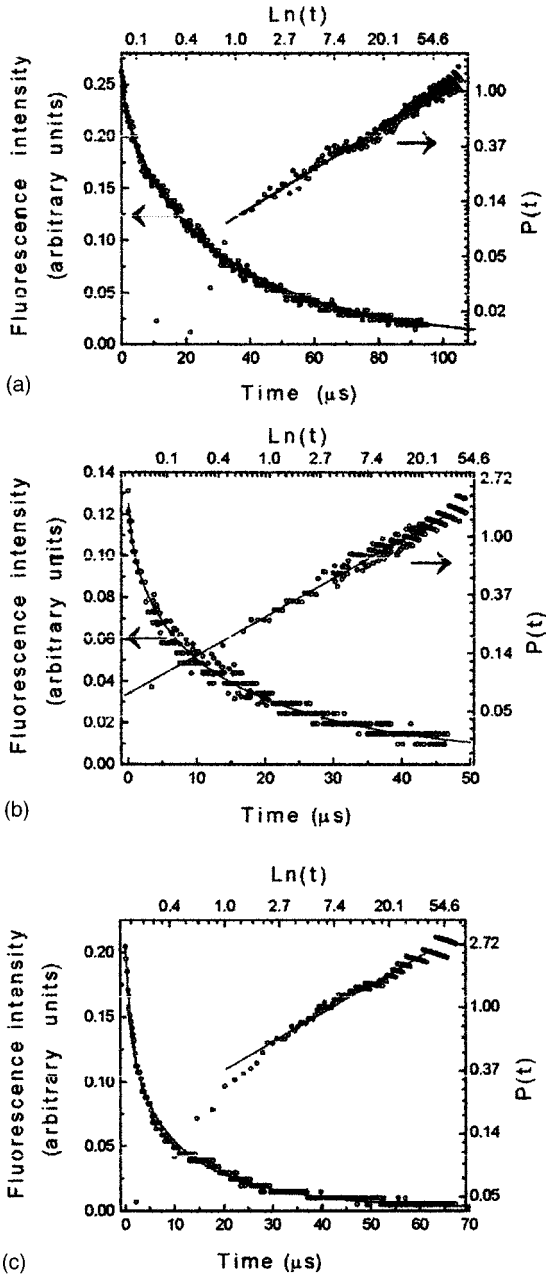

FIG. 5. Time dependence of $P(t)$ as determined monitoring the UC emission at 455 nm. Excitation wavelength: 650 nm. (a) sample concentration: $x = 1.0$; (b) $x = 2.0$; (c) $x = 3.0$. The solid line is a theoretical fitting based on the Inokuti-Hirayama model.

The proposed UC pathway is illustrated in Fig. 4 where it is indicated that the blue and UV emissions are due to a two-step one-photon absorption.

We recall that the cut-off phonons in the FIG matrix is ≈500 cm^{-1} and thus, the multiphonon relaxation rate between levels $^1D_2$ and $^1G_4$ is negligible. Energy transfer among Tm^{3+} ions is the main mechanism contributing to the lifetime of level $^1D_2$. The lifetime of the $^3H_4$ level is also dominated by processes of ion-ion interaction as in other glasses.[1,2,22]

When ET among the emitting atoms (donors) and traps of excitation (acceptors) occurs the fluorescence decay can be described by

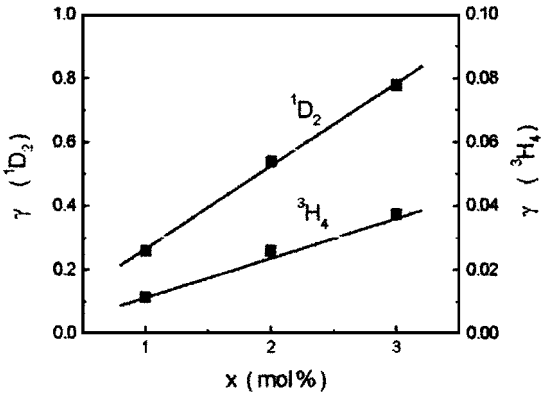

FIG. 6. Linear dependence of γ with Tm^{3+} concentration.

$$I(t) = 1_0 \exp\left(-\frac{t}{\tau_0} - P(t)\right), \tag{1}$$

where τ_0 is the lifetime of the isolated ions in the absence of ET. $P(t)$ is the transfer function which assumes different forms according to the sample concentration, origin of the interaction among the ions, and time range. $P(t)$ may have contributions due to ET processes which originate UC emissions, cross relaxation, and other processes between donors and acceptors that contribute to frequency downconversion emissions. Accordingly with the theoretical model of Inokuti and Hirayama[23] $P(t)$ is given by the expression

$$P(t) = \frac{4\pi R_0^3}{3} c\Gamma\left(1 - \frac{3}{s}\right)\left(\frac{t}{\tau_0}\right)^{3/s} = \gamma t^{3/s}, \tag{2}$$

where c is the concentration of acceptors and R_0 is the critical distance between Tm^{3+} ions at which the ET rate is equal to the decay rate of the donor ion, s is the parameter of the multipolar interaction [$s=6,8$, or 10 for dipole-dipole, quadrupole-dipole, and quadrupole-quadrupole interactions, respectively] and $\Gamma[1-(3/s)]$ is the Gamma function. The ET donor-acceptor can be of two types: (a) static transfer (ST), where the energy is transferred from an excited donor to an unexcited acceptor, and (b) fast diffusion, where the energy is transferred from an excited acceptor after migration to donors.[24] The ST process is expected to give the main contribution in our experiments because we have not observed pure exponential decay for any sample. Fast diffusion may be important for larger Tm^{3+} concentrations.

Figures 5(a)–5(c) illustrate the dynamical behavior of the blue emission at $\approx$455 nm with excitation at 650 nm for $x=1.0$, 2.0, and 3.0. The solid lines represent Eq. (1) fitted to the data points assuming $\tau_0=67$ μs, which is the value calculated using the J-O theory. An analogous procedure was employed for the other emissions.

To infer the kind of interaction between donors and acceptors the logarithm of $P(t)$ versus the logarithm of t was examined. The results, obtained by extracting an exponential part, $\exp(-t/\tau_0)$, from the recorded fluorescence signal, correspond to $P(t)\propto t^{\eta}$, with $0.48<\eta<0.59$. This behavior is also illustrated in Fig. 5. The value of $\eta\approx 0.5$ indicates that dipole-dipole interaction is the main mechanism for ET among the ions.

TABLE IV. Comparison between the critical distance R_0 and the average distance between the Tm^{3+} ions R_{av} obtained assuming a homogeneous spatial distribution of ions.

x	Emission (cm^{-1})	γ ($s^{-1/2}$)	R_0 (Å)	R_{av} (Å)
1.0	22 222	0.11	17	21
2.0	22 222	0.22	17	17
3.0	22 222	0.34	17	15
1.0	27 550	0.16	17	21
2.0	27 550	0.26	18	17
3.0	27 550	0.37	18	15
1.0	12 610	0.03	17	21
2.0	12 610	0.05	17	17
3.0	12 610	0.08	17	15

The parameter γ in Eq. (2) was determined for all samples and the results are presented in Fig. 6 which displays a linear dependence of γ with the Tm^{3+} concentration. From the data of Fig. 6 the values of R_0 were calculated and the results are presented in Table IV. A comparison between R_0 and the average distance among Tm^{3+} ions, R_{av}, obtained assuming a homogeneous distribution of ions, shows that the actual distribution of dopants is not homogeneous. Notice that there is a good agreement between the values of R_0 determined from the results related to $^3H_4$ and $^1D_2$ manifolds.

IV. CONCLUSIONS

In summary, we investigated the spectroscopic properties of Tm^{3+} doped FIG and characterized the main physical processes taking place when a pulsed laser at 650 nm is used as the excitation source. Frequency upconversion was observed from red to blue and ultraviolet. The interaction among Tm^{3+} ions revealed by nonexponential decay of transitions $^1D_2 \rightarrow {}^3F_4$, $^1D_2 \rightarrow {}^3H_6$, and $^3H_4 \rightarrow {}^3H_6$ was studied using the Inokuti-Hirayama procedure. The results indicate a dominant dipole-dipole interaction among Tm^{3+} ions. The data allowed us to determine the critical distance for different concentrations and show that the Tm^{3+} ions are not homogeneously distributed in the samples.

ACKNOWLEDGMENTS

This work was supported by the Brazilian Conselho Nacional de Desenvolvimento Cientifico e Tecnológico (CNPq) and Fundação de Amparo à Ciência e Tecnologia do Estado de Pernambuco (FACEPE). We also acknowledge B. J. P. da Silva for technical support.

[1] M. Yamane and Y. Asahara, *Glasses for Photonics* (Cambridge University Press, Cambridge, 2000).
[2] *Rare Earth Doped Fiber Lasers and Amplifiers*, edited by M. J. Digonnet (Marcel Dekker, New York, 1993).
[3] See, for example: C. B. de Araújo, A. S. L. Gomes, L. H. Acioli, G. S. Maciel, L. de S. Menezes, L. E. E. de Araujo, Y. Messaddeq, and M. A. Aegerter, in *Trends in Chemical Physics*, edited by R. D. Brown (Research Trends, Trivandrum, India, 1996), Vol. 4, p. 59, and references therein.
[4] L. E. E. de Araujo, A. S. L. Gomes, C. B. de Araújo, Y. Messaddeq, A. Flórez, and M. A. Aegerter, Phys. Rev. B **50**, 16219 (1994).
[5] G. S. Maciel, C. B. de Araújo, Y. Messaddeq, and M. A. Aegerter, Phys. Rev. B **55**, 6335 (1997).
[6] N. Rakov, G. S. Maciel, C. B. de Araújo, and Y. Messaddeq, J. Appl. Phys.

91, 1272 (2002).
[7]C. B. de Araújo, G. S. Maciel, L. de S. Menezes, N. Rakov, E. L. Falcão-Filho, V. A. Jerez, and Y. Messaddeq, C.R. Acad. Sci., Ser. IIc: Chim **5**, 885 (2002).
[8]L. de S. Menezes, G. S. Maciel, C. B. de Araújo, and Y. Messaddeq, J. Appl. Phys. **94**, 863 (2003).
[9]M. Dejenka, E. Snitzer, and R. E. Riman, J. Lumin. **65**, 227 (1995).
[10]I. R. Martin, V. D. Rodriguez, V. Lavin, and U. R. Rodriguez-Mendoza, J. Appl. Phys. **86**, 935 (1999).
[11]J. Azkargota, I. Iparraguire, R. Balda, J. Fernández, E. Dénoue, and J. L. Adam, IEEE J. Quantum Electron. **30**, 1862 (1994).
[12]S. Kishimoto and K. Hirao, J. Appl. Phys. **80**, 1965 (1996).
[13]A. Florez, V. A. Jerez, and M. Florez, J. Alloys Compd. **303-304**, 335 (2000).
[14]C. R. Mendonça, B. J. Costa, Y. Messaddeq, and S. C. Zilio, Phys. Rev. B **56**, 2483 (1997).
[15]D. F. de Souza, F. Batalioto, M. J. V. Bell, S. L. Oliveira, and L. A. O. Nunes, J. Appl. Phys. **90**, 3308 (2001).
[16]A. A. Andrade, T. Catunda, R. Lebullenger, A. C. Hernandez, and M. L. Baesso, J. Non-Cryst. Solids **273**, 257 (2000).
[17]B. R. Judd, Phys. Rev. **127**, 750 (1962).
[18]G. S. Ofelt, J. Chem. Phys. **37**, 511 (1962).
[19]K. Tanimura, M. D. Shinn, and W. Sibley, Phys. Rev. B **30**, 2429 (1984).
[20]R. M. Almeida, J. C. Pereira, Y. Messaddeq, and M. A. Aegerter, J. Non-Cryst. Solids **161**, 105 (1993).
[21]E. W. J. L. Oomen, J. Lumin. **50**, 317 (1992).
[22]E. W. J. L. Oomen, P. M. T. Le Gall, and A. M.A. Van Dongen, J. Lumin. **46**, 353 (1990).
[23]M. Inokuti and F. Hirayama, J. Chem. Phys. **43**, 1978 (1965).
[24]See, for example: *Laser Spectroscopy of Solids*, Topics in Applied Physics Vol. 49, edited by W. M. Yen and P. M. Selzer (Springer, Berlin, 1981).